Characterization of ambient aerosols in Mexico City during the MCMA-2003 campaign with Aerosol Mass Spectrometry ? Part I: quantification, shape-related collection efficiency, and comparison with collocated instruments

D. Salcedo, K. Dzepina, T. B. Onasch, M. R. Canagaratna, Q. Zhang, A. Rr.
Huffman, P. F. Decarlo, J. T. Jayne, P. Mortimer, D. R. Worsnop, et al.

**Atmospheric
Chemistry
and Physics
Discussions**

ACPD

5, 4143–4182, 2005

Mexico City aerosol
during MCMA-2003
using an AMS
– Part I

D. Salcedo et al.

Characterization of ambient aerosols in Mexico City during the MCMA-2003 campaign with Aerosol Mass Spectrometry – Part I: quantification, shape-related collection efficiency, and comparison with collocated instruments

**D. Salcedo[1,2], K. Dzepina[2,3], T. B. Onasch[4], M. R. Canagaratna[4], Q. Zhang[2],
J. A. Huffman[2,3], P. F. DeCarlo[2,5], J. T. Jayne[4], P. Mortimer[4,*], D. R. Worsnop[4],
C. E. Kolb[4], K. S. Johnson[6], B. Zuberi[6,**], L. C. Marr[6,***], L. T. Molina[6],
M. J. Molina[6], R. M. Bernabé[7], B. Cardenas[7], C. Márquez[7], J. S. Gaffney[8],
N. A. Marley[8], A. Laskin[9], V. Shutthanandan[9], and J. L. Jimenez[2,3]**

[1]Centro de Investigaciones Químicas, Universidad Autónoma del Estado de Morelos,
Cuernavaca, Morelos, Mexico
[2]Cooperative Institute for Research in the Environmental Sciences (CIRES), University of
Colorado at Boulder, Boulder, CO, USA
[3]Department of Chemistry and Biochemistry, University of Colorado at Boulder, Boulder, CO,
USA

Title Page

Abstract | Introduction

Conclusions | References

Tables | Figures

|◄ | ►|

◄ | ►

Back | Close

Full Screen / Esc

Print Version

Interactive Discussion

EGU

[4] Center for Aerosol and Cloud Chemistry, Aerodyne Research Inc., Billerica, MA, USA

[5] Program in Atmospheric and Oceanic Sciences, University of Colorado at Boulder, Boulder, CO, USA

[6] Department of Earth, Atmospheric and Planetary Sciences and Department of Chemistry, Massachusetts Institute of Technology, Cambridge, MA, USA

[7] Centro Nacional de Investigación Capacitación Ambiental, Instituto Nacional de Ecología, México D.F., Mexico

[8] Argonne National Laboratory, Argonne, IL, USA

[9] William R. Wiley Environmental Molecular Sciences Laboratory, Pacific Northwest National Laboratory, Richland, WA, USA

∗ now at: John Hopkins University, Baltimore, MD, USA

∗∗ now at: GEO2 Technologies, Woburn, MA, USA

∗ ∗ ∗ now at: Department of Civil and Environmental Engineering, Virginia Polytechnic Institute and State University, Blacksburg, VA, USA

Correspondence to: J. L. Jimenez (jlj@alum.mit.edu)

EGU

Abstract

An Aerodyne Aerosol Mass Spectrometer (AMS) was deployed at the CENICA Super-site, while another was deployed in the Aerodyne Mobile Laboratory (AML) during the Mexico City Metropolitan Area field study (MCMA-2003) from 31 March–4 May 2003 to investigate particle concentrations, sources, and processes. This is the first of a series of papers reporting the AMS results from this campaign. The AMS provides real time information on mass concentration and composition of the non-refractory species in particulate matter less than 1 μm (NR-PM$_1$) with high time and size-resolution. For the first time, we report field results from a beam width probe, which was used to study the shape and mixing state of the particles and to quantify potential losses of irregular particles due to beam broadening inside the AMS. Data from this probe show that no significant amount of irregular particles was lost due to excessive beam broadening. A comparison of the CENICA and AML AMSs measurements is presented, being the first published intercomparison between two quadrupole AMSs. The speciation, and mass concentrations reported by the two AMSs compared relatively well. The differences found are likely due to the different inlets used in both instruments. In order to account for the refractory material in the aerosol, we also present measurements of Black Carbon (BC) using an aethalometer and an estimate of the aerosol soil component obtained from Proton-Induced X-ray Emission Spectrometry (PIXE) analysis of impactor substrates. Comparisons of AMS + BC + soil mass concentration with other collocated particle instruments (a LASAIR Optical Particle Counter, a Tapered Element Oscillating Microbalance (TEOM) and a DustTrak Aerosol Monitor) are also presented. The comparisons show that the AMS + BC + soil mass concentration during MCMA-2003 is a good approximation to the total PM$_{2.5}$ mass concentration.

1. Introduction

The Mexico City Metropolitan Area field experiment (MCMA-2003) was an intensive 5-week campaign that took place in the spring of 2003 (31 March–4 May), with the goal of investigating the atmospheric chemistry of the MCMA, with particular focus on emissions quantification, gas-phase photochemistry, and secondary particulate matter formation. A focal point of the campaign was a highly instrumented "Supersite" located at the "Centro Nacional de Investigación y Capacitación Ambiental" (CENICA), in the south east of Mexico City. CENICA is located in the campus of the Universidad Autónoma Metropolitana-Itzapalapa (UAM-I), approximately 10 km southeast of the city center, and within a medium income residential and commercial area. The main local sources of pollutants are traffic and some small industries.

During the MCMA-campaign, we deployed an Aerodyne Quadrupole Aerosol Mass Spectrometer (Q-AMS) at CENICA. The AMS reports concentrations of non-refractory species in particles smaller than about 1 μm (NR-PM$_1$) with high time and size-resolution (Jayne et al., 2000; Jimenez et al., 2003a). A second AMS was operated inside the Aerodyne Mobile Laboratory (AML) that was also operated at CENICA when not in use for emissions monitoring or as a fixed site at other locations within the city (Kolb et al., 2004). In this paper we describe the AMSs' operation and calibration, and the first field measurement of the shape-related collection efficiency of the AMS. Also for the first time, we show an intercomparison between two collocated Q-AMSs. Finally, we report on intercomparisons between the AMSs and other collocated particle instruments deployed at CENICA (a LASAIR Optical Particle Counter, a Tapered Element Oscillating Microbalance (TEOM) and a DustTrak Aerosol Monitor). Since the AMS does not measure non-refractory aerosol components, we explicitly included in the total mass comparisons Black Carbon (BC) measurements provided by an aethalometer operated by the Argonne National Laboratory, and an estimation of the aerosol soil component from Proton-Induced X-ray Emission Spectrometry (PIXE) analysis of impactor substrates obtained by the Pacific Northwest National Laboratory (PNNL) and

the Massachusetts Institute of Technology (MIT). In the companion paper (Part II), we will discuss in detail the main characteristics of the time evolution of the concentration, composition, and size distribution of the NR-PM$_1$ measured with the AMS at CENICA.

2. Experimental

2.1. Aerodyne Aerosol Mass Spectrometer (AMS)

The AMS has been described in detail previously (Jayne et al., 2000; Jimenez et al., 2003a) so only a brief description will be given here. The AMS instrument consists of three main parts: an aerosol inlet, a particle sizing chamber, and a particle detection section. Particles are sampled from ambient pressure into ~1.5 Torr, and are focused using an aerodynamic lens into a narrow beam of ~100 μm diameter (Heberlein et al., 2001). The aerodynamic lens allows near unity transmission for particles in the size range of 60 nm to 600 nm, and partial transmission down to ~30 nm and up to ~1.5 μm. In the expansion at the exit of the lens into the high vacuum chamber the particles acquire a size-dependent velocity. The beam then passes through a spinning chopper wheel in the particle sizing chamber, where vacuum aerodynamic diameter (d_{va}) of the particles (Jimenez et al., 2003b; Jimenez et al., 2003c; DeCarlo et al., 2004) is determined by measuring the time it takes a particle to reach the detector (particle time-of-flight or P-ToF). In the detector the particle beam impacts on a heated surface (~600°C) under high vacuum (~10^{-7} Torr), leading to flash vaporization of the "non-refractory" (NR) particle species. NR is defined operationally to include all species that evaporate in a few seconds under these conditions. In practice NR includes species such as ammonium sulfate and sodium nitrate, and excludes black carbon, crustal materials, and sea salt/sodium chloride. Non-refractory species internally mixed with refractory species (e.g. organics internally mixed with black carbon) can be quantitatively detected with the AMS (Katrib et al., 2005; Slowik et al., 2004). The NR particle species that are vaporized at the heated surface are then subjected to electron impact

(EI) ionization, which forms positive ions that are analyzed with a quadrupole mass spectrometer. The signal is linear with particle mass of a given species and detection limits below $1\,\mu g\,m^{-3}$ are typically achieved for all species (see Sect. 2.4.1).

During the MCMA campaign, a recently developed beam width probe (BWP) was used with the AMS to provide a continuous measurement of surrogate particle morphology (non-sphericity) and to allow the estimation of the potentially reduced particle collection efficiency due to particle shape. The design of the probe and the techniques for analysis and interpretation of its data have been extensively discussed elsewhere (Jayne et al., 2000; Huffman et al., 2005[1]). The probe used in this study consisted of a 0.41 mm diameter wire, which was moved intermittently to a fixed position blocking part of the particle beam near the AMS vaporizer in order to determine the attenuation of the signal vs. wire position. The BWP was alternated between the "out" position (not blocking any part of the vaporizer) and one of the seven partially blocking positions in front of the 3.81 mm diameter vaporizer. One of the seven blocking positions covered the center of the vaporizer and six were symmetrically located around the center to each side, with partial vaporizer blocking. The probe was operated in two-minute intervals, with a total cycling time (loop through the entire round of positions) of 28 min.

2.2. CENICA AMS operation

The AMS was located inside a hut built on the roof of the 12 m tall building that houses CENICA. Ambient air was sampled at a flow rate of 9 lpm through a $PM_{2.5}$ cyclone (URG-2000-30EN, URG, Chapel Hill, NC) located 2.3 m above the roof of the hut and drawn into a 9.525 mm (3/8 inch) copper tubing to within 15 cm of the AMS inlet, where 8.9 lpm were exhausted by a vacuum pump and ~0.1 lpm was sampled into the AMS from the center of the 9.525 mm line. The total length of the inlet line was 5.3 m.

[1]Huffman, J. A., Jayne, J. T., Drewnick, F., Aiken, A. C., Onasch, T., Worsnop, D. R., and Jimenez, J. L.: Design, Modeling, Optimization, and Experimental Tests of a Particle Beam Width Probe for the Aerodyne Aerosol Mass Spectrometer, Aerosol Sci. Technol., submitted, 2005.

Maximum particle losses due to diffusion and bends in the line were calculated (Baron and Willeke, 2001) to be 6.5% for 30 nm particles and 0.7% for 1 μm particles.

The ions chosen and the main species monitored with the AMS P-ToF mode during this campaign were: m/z 16 for ammonium (NH_2^+); m/z 18 for water (H_2O^+); m/z 28 for the airbeam (N_2^+); m/z 30 and 46 for nitrate (NO^+, NO_2^+); m/z 36 for chloride (HCl^+); m/z 48 and 64 for sulfate (SO^+, SO_2^+); m/z 43, 44, 55, 57, 67, 77, and 141 for organic species; and m/z 202 and 226 for polycyclic aromatic hydrocarbons (PAHs).

The various BWP blocked positions and the unblocked position were alternated every two minutes. This produced a 4-min, 50% duty cycle dataset without the BWP that is used to derive particle concentrations in this paper. The combination of this unblocked dataset with the other interleaved, 4-min, 50% duty cycle of BWP data for the seven blocked positions is analyzed in Sect. 3.1 to determine the shape-related collection efficiency (see Sect. 2.4 for its definition).

All mass concentrations presented in this paper for all instruments are at ambient temperature and pressure conditions (local pressure is approximately 76 kPa). Local Standard Time in Mexico City normally corresponds to Central Standard Time (CST) or Coordinated Universal Time (UTC) minus 6 h. On 6 April 2003 at 02:00 a.m. the Daylight Savings Time period started in Mexico; after that, local time corresponded to Central Daylight Saving Time (CDT) or UTC minus 5 h. All data in this paper is reported in Local Time, i.e. CST before 6 April and CDT after 6 April.

2.3. Mobile Laboratory AMS operation

A second AMS, also equipped with a BWP, was operated on-board of the Aerodyne Mobile Laboratory (Kolb et al., 2004). The AML was stationed at CENICA while not in use for "vehicle chase" experiments (Canagaratna et al., 2004), vehicle fleet emissions measurements, ambient pollutant mapping activities, or as a high time resolution fixed site in other locations across Mexico City (Kolb et al., 2004). The design and operation of both AMSs was the same, with the exception of the use of a smaller critical orifice for sampling from ambient pressure in the AML AMS (100 μm in the AML AMS vs 120 μm

in the CENICA AMS). The smaller AML AMS orifice was selected to favor the transmission of smaller particles expected for fresh vehicle exhaust in the AML AMS during vehicle chase experiments since it is known that the window of particle sizes transmitted shifts to slightly smaller sizes as the lens operating pressure decreases (Zhang et al., 2004b). This led to slightly different particle transmission functions between the two AMSs.

2.4. AMS quality control and calibrations

2.4.1. AMS ionization efficiency calibration

The ionization efficiency (IE) of both AMSs was calibrated every few days with dry monodisperse NH_4NO_3 particles with the procedure described previously (Jimenez et al., 2003a; Zhang et al., 2005b). Figure 1 shows the results of all IE calibrations for the CENICA and AML AMSs during the campaign.

Panels (a) and (d) of Fig. 1 show the airbeam signal (m/z 28 signal from gas phase nitrogen, N_2, sampled from ambient air) for the two AMSs. Fluctuations in the airbeam signal reflect changes in atmospheric pressure (the changes are minor for typical synoptic weather patterns, but significant for altitude changes) and the fundamental sensitivity of the AMS ionization and mass analysis techniques. The sensitivity of the AMS can change due to changes in the electron multiplier gain, significant changes in inlet alignment, changes in the sampling orifice, and, most importantly, changes in the ionization, extraction, and detection efficiencies. The airbeams shown in Fig. 1 indicate an absolute change of less than 20% for either AMS over the whole campaign.

The ionization efficiency calibrations of the AMSs are shown in panels (b) and (e) of Fig. 1 and represent the ratio of the number of ions measured at m/z 30 and 46 for the NO^+ and NO_2^+ fragments of NH_4NO_3 to the total number of NH_4NO_3 molecules in a monodisperse aerosol sampled by the AMS. Thus, this calibration includes the ion detection sensitivities inherent in the airbeam measurement plus the additional sensitivities to vaporization, and ionization of particle chemical components. The accuracy

of the AMS measurements during MCMA-2003 was partially limited by our ability to calibrate the ionization efficiencies. The efficiency with which various chemical species ionize in the AMS is calculated by multiplying the calibrated nitrate IE values by the appropriate relative ionization efficiencies (RIE) factors. The MCMA data was analyzed using previously published RIEs of 1.2 for sulfate, 1.1 for nitrate, 1.4 for organics and 1.3 for chloride (Jimenez et al., 2003a; Alfarra et al., 2004). The NH_4NO_3 IE calibration allows for the direct determination of the ammonium RIE. The ammonium RIE measured for the CENICA the AML AMSs were 3.8–6.2 and 4.5, respectively.

The IE calibration results shown in Fig. 1 for both of the instruments exhibit more scatter than the airbeam measurements. This scatter represents the uncertainty inherent in accurately generating and sampling a known number of molecules of ammonium nitrate in aerosol form. The two AMS instruments were typically calibrated with operators from both instruments and the aerosol generation system was shared between the two groups. During the study, a new IE calibration procedure was adopted after 13 April, which relied on sampling polystyrene latex spheres (PSLs) to provide a more accurate size measurement for the subsequently sampled monodisperse ammonium nitrate aerosol. The IE calibrations were reasonably constant for the CENICA AMS, but exhibited a significant decrease with time for the AML AMS. The CENICA AMS was stationary during the duration of the study, whereas the AML AMS was operated on the roads in chase mode during most days of the study and was stationary during nights and several specific time periods at remote locations around the Mexico City Metropolitan Area. The decrease in the AML AMS IE is most likely due to an inlet alignment change caused by abrupt motions experienced by the AMS during on-road operations.

The true calibration of the AMS for quantitative particle chemical composition is determined by the ratio of the IE/AB values. The IE/AB ratio for both instruments is shown in panels (c) and (f) of Fig. 1. The symbols show the measured values and the solid line shows the IE/AB calibration values used to correct the mass loading data. The IE/AB reference values for the CENICA AMS were nearly constant, especially after the new

calibration procedure was adopted, and a constant value of 6.57×10^{-13} was chosen to correct the complete data set, except for the final three days. During the final few days of the study, the CENICA AMS experienced a malfunction of an internal component whose replacement required the instrument losing vacuum. Due to time and personnel constraints, an IE/AB calibration was not performed on this instrument after the failure. Given the good agreement between both AMSs for the rest of the campaign, the IE/AB value used for this period for the CENICA AMS was chosen by comparison with co-located AML AMS data, which suggested the apparent change in the IE/AB value for this period. In contrast, IE/AB values for the AML AMS show a strong decrease during the first half of the study and only settle out during the second half of the study, following the same pattern observed in the individual IE measurements.

The detection limits (DLs) from individual species were determined by analyzing periods in which ambient filtered air was sampled and are reported as three times the standard deviation (3σ) of the reported mass concentration during those periods. DLs during this campaign for the CENICA based AMS were 0.01, 0.09, 0.11, 0.41 and 0.04 μg m^{-3} for nitrate, sulfate, ammonium, organics and chloride respectively for a 10 min. averaging time. The DLs for the Mobile Laboratory based AMS were 0.04, 0.06, 0.2, 0.8 and 0.04 μg m^{-3} for nitrate, sulfate, ammonium, organics and chloride respectively for a 10 min. averaging time. These DLs are similar between the two instruments and close to those reported for previous AMS campaigns (Zhang et al., 2005b).

2.4.2.   Analysis of Potential Interferences in the AMS Measurements

The quadrupole AMS (Q-AMS) used in this study operates with unit m/z resolution. Since multiple ions can produce signals at the same integer m/z, there is no direct way to separate their contributions based on Q-AMS data. E.g. NO+, CH$_2$O$^+$, and/or C$_2$H$_6^+$ can produce signals at m/z 30 and these signals are indistinguishable when recorded. Allan et al. (2004b) have developed a linear deconvolution procedure to ap-

portion the signals recorded at each integer m/z of the Q-AMS into species-specific spectra based on observed fragmentation patterns in laboratory and calibration experiments, and on element isotopic ratios. This algorithm has been implemented in the standard AMS analysis software used for the analyses presented here. However it is still possible that some interferences may remain if they do not fit the patterns assumed in the "fragmentation tables" that are used with the algorithm. Jimenez et al. (2003a) introduced a procedure to check for such interferences by examining the correlation between the time series and the size distributions of several ion fragments attributed to the same inorganic species. Since an interfering species will likely not be correlated in time with a given inorganic species, owing to likely differences in sources and formation processes, deviations in the correlation of the different fragments can be indicative of remaining unsubtracted interferences. Conversely, the lack of deviations in these correlation plots is a necessary, although not sufficient condition for lack of major interferences. Figure 2 shows the correlation between the time series of the main ion fragments used to calculate the mass concentration of the inorganic species during the MCMA-2003 study. Note that the AMS concentration of a given species is obtained by summing the individual concentrations of the ions it produces (Jimenez et al., 2003a). The mass concentrations of individual ions, such as nitrate at m/z 30, are an intermediate step in the calculation of the species mass concentrations and are proportional to the ion signals, but do not have a direct physical meaning in terms of "concentration of a fragment" in ambient air. Although there is significant scatter in the time series plots, likely owing to limited-signal to noise of the individual measurements, there is no clear sign of significant deviations from linearity. This indicates that unsubtracted interferences from organic fragments in the retrieved concentrations of the inorganic species are small during this campaign. A small exception may be the small deviations in the correlation between the nitrate fragments in the different periods, which may be due to the presence of small concentrations of organic nitrates.

2.4.3. Calculation of the AMS mass concentration

In previous studies using the AMS (Allan et al., 2004a; Drewnick et al., 2004a; Hogrefe et al., 2004; Zhang et al., 2005b), it has been observed that there is a systematic (but generally highly reproducible) underestimation of the mass concentration of aerosols measured with the AMS when compared to other quantitative aerosol measurements such a the Particle Into Liquid Sampler (PILS). In these studies, the underestimation in mass concentration observed with the AMS indicates AMS Collection Efficiencies (CE) ranging from 0.43 to 1.

Huffman et al. (2005[1]) have recently defined the observed AMS collection efficiency in terms of three terms: $CE = E_L * E_s * E_b$. The E_L term accounts for the portion of $PM_{2.5}$ that is not transmitted into the AMS due to the approximate PM_1 size cut (Jayne et al., 2000; Zhang et al., 2005b) of the aerodynamic lens in the AMS. The latter two terms account for possible effects that cause the PM_1 particles that are introduced into the instrument and get through the aerodynamic lens to still not be detected by the mass spectrometer. The shape-related collection efficiency (E_s) could be less than one for nonspherical particles because the efficiency with which they are focused by the lens is reduced (Jayne et al., 2000; Huffman et al., 2005[1]) and this in turn could potentially cause irregular particles to "miss" the AMS vaporizer. The bounce-related collection efficiency (E_b) could be smaller than one if dry less-volatile particles such as those with a high proportion of $(NH_4)_2SO_4$, bounce after impacting the AMS vaporizer, instead of evaporating. Previously, the latter two effects (and sometimes all three effects) had been included in one collection efficiency ($CE = E_s * E_b$) (Alfarra et al., 2004; Drewnick et al., 2004b; Zhang et al., 2005b).

The newly developed beam width probe (BWP) that was operated in this campaign allowed for the first direct measurements of E_s in the field. In Sect. 3.1, we show that $E_s \sim 1$ during this field campaign. E_b is more difficult to determine because it likely depends on particle phase (liquid vs. solid), water content, and particle composition. Particles with significant ammonium sulfate content appear to bounce with $E_b \sim 0.5$ when

they are dry inside the AMS, and to be collected with $E_b \sim 1$ when they retain water after entering the vacuum system (Hogrefe et al., 2004). Pure ammonium nitrate and ammonium nitrate-dominated ambient particles are collected with $E_b \sim 1$ (Jayne et al., 2000). The evidence is less clear for organic-dominated particles, as was the case during most of the MCMA-2003 campaign. Observations of ambient particles dominated by oxygenated organic aerosol (OOA) off the coast of New England, showed a $E_b \sim 0.5$ (Onasch et al., 2005[2]). Chamber experiments have also shown that secondary organic aerosols (SOA) formed from photooxidation of aromatics, and from ozonolysis of biogenic compounds, have an $E_b \sim 0.5$ (Bahreini et al., 2005). Since analysis of the submicron aerosol in Mexico City shows that a large fraction is OOA, likely mostly SOA from the photooxidation of aromatics and other precursors (Dzepina et al., 2005[3]), a similar value may be applicable to this study.

Given the evidence and uncertainties from previous laboratory studies and field campaigns, we have chosen a value of $E_b = 0.5$ for all species for this campaign. We estimate the maximum range of possible values of this parameter between about 0.45 and 0.70. Thus the mass concentrations reported in this paper have a range of uncertainty of about −30% and +10% due to the uncertainty in particle collection efficiency. The comparisons with other instruments presented in Sect. 3.3 are also consistent with the value of CE chosen here. Despite the uncertainty in the absolute concentrations, the relative variation in concentrations and size distributions reported here have a lower uncertainty, as evidenced by the fact that the dynamics of the AMS and TEOM/DustTrak/LASAIR concentrations track each other during the campaign (see Sect. 3.3).

---

[2]Onasch, T. B. et al.: AMS measurements off the coast of New England, in preparation, 2005.

[3]Dzepina, K. et al.: The Organic Aerosol during MCMA-2003, in preparation, 2005.

2.5. Collocated aerosol instrumentation

2.5.1. Black carbon measurements

The black carbon content of fine aerosols was estimated from the aerosol light absorption using a seven-channel aethalometer (RTAA-1000, Magee Scientific, Berkeley, CA). Its sampling line was found to effectively collect aerosols in the 0.1 to 2.0 micron size range (PM_2). The particles are collected within the instrument by continuous filtration through a quartz filter tape strip. The optical transmission of the deposited aerosol particles is then measured sequentially at seven wavelengths (370, 450, 520, 590, 660, 880, and 950 nm). Black carbon is a strongly absorbing component whose light absorption coefficient is relatively constant over a broad spectral region. The instrument automatically calculates the black carbon concentration from the transmission measurements by assuming black carbon to be the main absorbing aerosol species in the samples with a mass specific absorption coefficient of $19\,m^2\,g^{-1}$ (Hansen et al., 1982; Marley et al., 2001). This value is larger than those typically used for the absorption of black carbon suspended in air due to the enhancement of the particle absorption in the fiber matrix of the filter tape (Anthony Hansen, Magee Scientific, personal communication). Data were recorded for each of the seven channels at a two-minute time resolution. In addition, the analog output of the 520 nm channel was monitored continuously and one minute averages of this channel were recorded separately. As the sample is deposited on the paper tape strip, the light attenuation steadily increases. At high sample loadings the high absorptions cause detection limits to decrease. To prevent this, the instrument automatically advances the tape to a new sample spot when light attenuation becomes severe. The instrument sample was diluted 10:1 to minimize the instrument down time created by too frequent tape advances due to the high black carbon loading observed in Mexico City.

Unlike other absorbing aerosol species (e.g. humic like substances), black carbon absorption is relatively constant from the ultraviolet to the infrared (Marley et al., 2001). Thus a comparison of results from the different channels can act as an independent

Title Page

Abstract   Introduction

Conclusions   References

Tables   Figures

◄   ►►

◄   ►

Back   Close

Full Screen / Esc

Print Version

Interactive Discussion

Mexico City aerosol during MCMA-2003 using an AMS – Part I

D. Salcedo et al.

validation of the assumption that black carbon is the main absorbing species in the samples. For the sampling period, all seven channels were found to be in excellent agreement, with a variation of 1–2%, indicating that black carbon was indeed the major light absorbing material present in the aerosol, if not the only one. The results from the
5 880 nm channel are used in this paper.

Jeong et al. (2004) reported that measurements of BC using an aethalometer can be up to about a factor of three different (higher or lower) than simultaneous measurements of elemental carbon (EC) using a thermal-optical method, depending on the physical and chemical characteristics of light absorbing species in the particles. Be-
10 cause of this, there is some uncertainty on the actual EC/BC mass concentrations in Mexico City during the MCMA-2003.

2.5.2. Impactor aerosol collection and PIXE analysis

A detailed description of the impactor sampling and analysis techniques are given elsewhere (Johnson et al., 2005a[4]) (Shutthanandan et al., 2002), hence only a brief
15 description is presented here. Impactor aerosol collections were made continuously onto Teflon strips with a 3-Stage IMPROVE DRUM impactor (UC Davis, California) in size ranges 1.15–2.5 μm, 0.34–1.15 μm, and 0.07–0.34 μm. The DRUM was operated with a fixed flow rate of 10 SLPM and rotation of 2 mm per 12 h. Proton-Induced X-ray Emission (PIXE) analysis was carried out immediately following the campaign at
20 the Environmental Molecular Sciences Laboratory (EMSL), a national scientific facility within Pacific Northwest National Laboratory located in Richland, WA. A 3.5 MeV proton beam with diameter 0.5 mm was used during analysis. PIXE spectra were interpreted with the GUPIX program (Maxwell et al., 1995) and concentrations of elements Na to Pb determined by calibration to known standards. Concentrations are given in
25 6-h averages.

---

[4]Johnson, K. S. et al.: Composition and Sourcing of Aerosol in the Mexico City Metropolitan Area with PIXE/PESA/STIM and Multivariate Analysis, in preparation, 2005a.

The soil particulate mass concentration is estimated from PIXE mass concentrations using the method described by Malm et al. (1994). These authors estimate the soil particulate mass concentration by summing the elements predominantly associated with soil, plus oxygen for the most common oxides (Al_2O_3, SiO_2, CaO, FeO, Fe_2O_3, TiO_2), plus corrections for other compounds such as K_2O, MgO, Na_2O, water and carbonate. The equation used is:

$$[soil]=2.20[Al] + 2.49[Si] + 1.36[Ca] + 2.42[Fe] + 1.94[Ti] \tag{1}$$

2.5.3. Other particle instruments

A LASAIR Optical Particle Counter model 1001 (Particle Measuring Systems, Boulder, CO), and a DustTrak Aerosol Monitor model 8520 (TSI, St. Paul, MN) were deployed at the CENICA site by the MIT and PNNL research groups.

The LASAIR device detects light scattered by individual particles crossing a detection volume illuminated with laser light and estimates the particles size by assuming that the scattered light intensity is a monotonic function of the particle size (Hinds, 1999). It determines the number concentration of particles in 8 different size channels (0.1–0.2 μm, 0.2–0.3 μm, 0.3–0.4 μm, 0.4–05 μm, 0.5–0.7 μm, 0.7–1.0 μm, 1.0–2.0 μm, 2.0–5.0 μm; equivalent geometric diameter, d_p). The nominal detection efficiency is 100% for all channels, with the exception of 50% for the smallest channel.

The DustTrak is an aerosol photometer that uses a laser-beam to illuminate a sample stream, in which multiple particles scatter light in all directions. A detector determines the total amount of light scattered at a 90 degree angle, which is roughly proportional to the mass concentration of the aerosol (TSI, 2004). The DustTrak deployed during the MCMA campaign used a $PM_{2.5}$ impactor inlet. The DustTrak measurement was calibrated with gravimetric filter measurements taken by CENICA during the MCMA-2003 campaign and agreed well with a similar unit on board of the Aerodyne Mobile Lab when parked at CENICA.

A Tapered Element Oscillating Microbalance (TEOM, Rupprecht & Patashnick, East

Greenbush, NY), which measures total $PM_{2.5}$ mass concentration was operated by CENICA. The TEOM measures the $PM_{2.5}$ total mass concentration using a vibrating element, whose resonant frequency depends on the accumulated particle mass collected on a filter located at the extreme of the element (Hinds, 1999). The TEOM used during the MCMA-2003 operated at 35°C and was not equipped with a Sample Equilibration System (SES).

3. Results and discussion

3.1. Determination of the Shape-Related Collection Efficiency (E_s)

The average signal attenuation measured for each species as a function of BWP position across the particle beam is shown in Fig. 3. Chloride is not included because its concentration was very low most of the time and the attenuated signal profile is very noisy. The attenuation at each position is similar for all species, and it is large only when the BWP is at the center position. This means that on average the particle beam is well-focused on the vaporizer. By applying the model of Huffman et al. (2005)[1] to the time dependent attenuation profiles of all species we estimate that $E_s \sim 1$ for all species during this field campaign; i.e., no significant particle mass goes undetected because of excessive beam divergence caused by particle non-sphericity. The fact that the profiles of all species are similar suggests internal mixing of the species most of the time, since externally mixed particles would likely have different profiles for different species. Similar conclusions were obtained from the analysis of the speciated size distributions (Salcedo et al., 2005), and with electron microscopy studies of individual particles collected at the CENICA site (Johnson et al., 2005b). The airbeam signal is attenuated at all positions except the outermost one, which indicates that the airbeam is not as well-focused as the particle beam. The attenuation of the airbeam is not symmetrical around the center of the heated surface, which is probably due to slight imperfections of the several apertures and skimmers that this beam traverses inside the AMS.

Particle beam focusing in aerodynamic lenses is known to be a function not only of shape, but also of particle size (Zhang et al., 2004b; Huffman et al., 2005[1]). In order to explore the focusing of the ambient particle beam as a function of particle size, panels (a) through (d) in Fig. 4 show the size distribution for each species compared with the size distribution measured when the BWP was blocking the center of the particle beam. Panels (e) and (f) in Fig. 4 show the signal attenuation when the BWP was on the center position as a function of particle size. Note that the NH_4^+ attenuation profiles are noisier than for other species due to the higher noise for this species in the AMS, mainly due to interference from O^+ ions from O_2 and water. The signal attenuation reveals a size dependency: the smaller particles show lower attenuation in the presence of the BWP, which means that they are less well focused than the particles at the peak of the size distribution. This is expected since Brownian motion and the lower efficiency of aerodynamic focusing for small particles cause increased beam broadening for these particles, even if they are spherical, eventually leading to incomplete collection below ~60 nm (Zhang et al., 2002, 2004b). In addition, the ultrafine particle mode is dominated by combustion emissions in Mexico City (Dzepina et al., 2005[3]); hence, because they are likely internally mixed with soot, they are irregular. Non spherical particles, which are less focused by the aerodynamic lens (Liu et al., 1995; Jayne et al., 2000; Huffman et al., 2005[1]), form a wider beam and their signal should be attenuated less by the BWP. Although particle losses due to beam broadening for smaller particles can be considerable, we did not attempt to correct for this effect due to the complexities and assumptions needed, and because there are other uncertainties that are more important, such as the value of E_b (see Sect. 2.4). Particles in the accumulation mode (300–800 nm) show much larger attenuation, indicating that they are better focused. Particles larger than 1 μm have broader beams than those around 500 nm, as expected due to the reduced focusing ability of the lens for larger sizes (Zhang et al., 2004b). The similar attenuation for all species for the accumulation mode is also suggestive of internal mixing most of the time for this mode.

Figure 5a compares the mass concentration of total AMS NR-PM$_1$ (when the BWP

Mexico City aerosol during MCMA-2003 using an AMS – Part I

D. Salcedo et al.

did not block the particle beam at all) with the concentration measured when the BWP was blocking the center of the particle beam. Only a few days of the campaign are shown because the purpose of the figure is to illustrate the range of variation of this measurement, and the patterns were similar during other periods. Mass concentra-
5 tions in this figure were not corrected for air beam (AB) signal variations (Allan et al., 2003) because of the large variations in the AB were caused by the presence of BWP and that are not due to changes in the sensitivity of the instrument as assumed by the AB correction. Panel (b) shows the signal attenuation caused by the BWP at the position that blocks the center of the particle beam, compared to the non-blocking position
10 measurements in the 2 min preceding and following the attenuated measurement. The figure shows that the degree of attenuation of the signal has some variability in time, indicating changes in the particle beam focusing which might be attributed to changes in the particle shape. The shape-related collection efficiency, E_s, remained at 1 during this period. In order to explore the relationship between particle shape and the signal atten-
15 uation with the BWP, Fig. 5b also shows the signal of the ion fragment m/z 44, which is a marker for oxygenated organic aerosol (OOA) (Zhang et al., 2005a). The presence of OOA in the particles might be an indication of particle aging. Figure 5 shows that some of the variability in the signal attenuation appears to correlate with changes in the particle OOA concentration. However, this correlation does not always hold. Simi-
20 lar analyses to that exemplified by Fig. 5 were carried out using other parameters that may be correlated with particle sphericity or non-sphericity, such as relative humidity, particle size, black carbon, and hydrocarbon-like organic compounds (HOA, likely primary combustion aerosol) as indicated by the AMS ion fragment m/z 57. These correlations were also analyzed for selected AMS size ranges, since particle focusing
25 is also dependent on particle size. Various periods of correlations, anti-correlation, and no correlation between beam attenuation and these parameters were observed in the data from this campaign. However, no consistent trend was observed, indicating that multiple parameters may affect the average particle non-sphericity in a complex way. In order to understand this issue, detailed laboratory work with particles of known

sizes and shapes (e.g. combined with off-line electron microscopy measurements) and fieldwork at more locations need to be performed.

3.2. Comparison between AMSs

Figure 6 panels (a) and (b) show the comparison (time series and scatter plot) of the total NR-PM$_1$ measured with the CENICA and the AML AMSs for periods when the AML was parked at CENICA during MCMA-2003. Panels (b)–(f) show the scatter plots of the main NR-PM$_1$ species measured with both AMSs. The comparison is made using 30 min averages in order to minimize the effects of local plumes. While the two AMSs were co-located at CENICA, they were situated 20–50 m apart (parking lot and top of building) and were not sampling from the same inlet. Thus, either instrument could and was influenced by local, small scale (car, truck, industrial) plumes that were either sampled by the other AMS at a slightly different time, or not at all. Despite the slight difference in location, the correlations between the two AMSs for total NR-PM$_1$ and for each individual chemical component are generally good, exhibiting r^2 values greater than 0.84. Absolute magnitude differences between instruments were 14%, 32%, 17%, 12% and 1% for total, nitrate, sulfate, ammonium, and organics, respectively. The positive difference in the signals (CENICA > AML) for the total and each individual species, with the apparent exception of the organics, is due to the different inlets used in the CENICA and AML AMSs. The largest difference (32%) is noted in the nitrate comparison and occurred on 9 and 10 April, depicted as the yellow time period in Fig. 6. During this period, the aerosol composition was dominated by nitrate and organics and to a less degree, ammonium and sulfate. The median diameters of the accumulation mode of the nitrate and organics size distributions during this period (513 and 476 nm, respectively) were larger than the median diameter for the nitrate and organics during the full campaign (438 and 343 nm, respectively) (Salcedo et al., 2005). Measurements with LASAIR further confirm that the particles size distribution shifts to larger diameters during this period. Since a 120 micron orifice allows larger particle transmission compared with the 100 micron orifice, the AML AMS was missing

a fraction of the mass measured by the CENICA AMS during 9 and 10 April. This effect is readily apparent in the correlation plots in Fig. 6, where the yellow points in the total, nitrate, sulfate, ammonium, and organics comparisons are all higher than the 1:1 line. The reason for the small magnitude difference in the case of the organics is due to the
5 fact that the fit is dominated by higher organic concentrations measured at a different time.

3.3.   Comparison with collocated particle instruments

The DustTrak and TEOM measure the total particulate concentration, including both refractory and non refractory species. In order to properly compare these instruments
10 to the AMS, the mass of the refractory species needs to be added to the total AMS non-refractory mass concentrations. Thus we have added the AMS, BC, and estimated soil particulate mass concentrations as the best approximation to the total particle mass concentration from the sum of all speciated measurements. This correction to the AMS data is important for the comparison with other instruments because the BC + soil mass
15 concentration was relatively high during the MCMA-2003 (equivalent to ~20% of the Total NR-PM$_1$, (Salcedo et al., 2005)). Figure 7 shows the comparison of AMS + BC + soil mass concentration with that measured by the DustTrak and TEOM. For the TEOM only a few days at the end of the campaign were available due to instrument malfunction in the earlier part. Scatter plots between the three data sets are also shown in
20 Fig. 7. Note that the AMS measured approximately PM$_1$, while the aethalometer measured PM$_2$ BC, and the impactor subtracts, DustTrak and TEOM measured PM$_{2.5}$. The total AMS + BC + soil concentrations are close on average to the total PM$_{2.5}$ mass measured by either TEOM or DustTrak. The agreement between AMS + BC + soil concentrations and the other total mass measurements suggests that there is very
25 little non-refractory mass in particles with diameters between 1 and $2.5\,\mu$m. These observations can be further substantiated by analyzing the size distribution data provided by the LASAIR.

The size distributions of the LASAIR measurements and the combined AMS + BC

+ soil mass loadings are compared in Figure 8 (note the different scales). The black carbon size distribution was estimated using the size distribution of ion fragment m/z 57, which has been used as a marker for fresh primary emitted particles; thus, it is expected to have a similar size distribution as black carbon vs. vacuum aerodynamic diameter (Zhang et al., 2005a, b). The size distribution of AMS fragment m/z 57 was scaled so that the integrated mass concentration was equal to the BC mass concentration. The number concentration of particles in each LASAIR channel was converted to volume concentration assuming that the particle probability density is constant for all sizes in each bin. Then, we converted the particle volume concentration into mass concentration by multiplying the volume by the estimated size dependent material density (ρ_m, g cm^{-3}), calculated using the following equation (DeCarlo et al., 2004):

$$\rho_m = \frac{[NO_3^-] + [SO_4^{2-}] + [NH_4^+] + [Cl^-] + [\text{organics}] + [BC] + [\text{soil}]}{\frac{[NO_3^-]+[SO_4^{2-}]+[NH_4^+]}{1.75} + \frac{[Cl^-]}{1.52} + \frac{[\text{organics}]}{1.2} + \frac{[BC]}{1.77} + \frac{[\text{soil}]}{2.7}} \quad (2)$$

where [NO$_3^-$], [SO$_4^{2-}$], [NH$_4^+$], [Cl$^-$], [organics], [BC], and [soil] represent the size dependent mass concentration of each species. Equation (2) assumes that the densities of ammonium nitrate, ammonium sulfate, and ammonium bisulfate are approximately 1.75 g cm^{-3} (Lide, 1991); the density of ammonium chloride is 1.52 g cm^{-3} (Lide, 1991); the density of organics is 1.2 g cm^{-3} (Turpin and Lim, 2001); the density of black carbon 1.77 g cm^{-3} (Park et al., 2004); the average density of soil, calculated from the weighted average density of the main oxides (Lide, 1991), is 2.7 g cm^{-3}. The d_{va} corresponding to the geometric diameter (d_p) of each channel boundary of the LASAIR and the impactor substrates, was also calculated from d_p using the estimated size-dependent density (Jimenez et al., 2003b).

Figure 8 shows that the LASAIR measured lower mass concentrations than the AMS + BC + soil. The discrepancy may be partially due to saturation of the LASAIR with the high particle number concentrations in Mexico City. This instrument has some electronic dead time after counting each particle, and must be used with a diluter to avoid

this saturation effect (Murphy et al., 1997), but unfortunately a diluter was not used during this study. The average aerosol number concentration reported by the LASAIR for its size range during MCMA-2003 was 1922 cm^{-3}; almost an order of magnitude higher than the maximum ambient concentration recommended for the LASAIR 1001 (353 cm^{-3}). This very likely caused the instrument to undercount particles. An undercounting effect has been observed in other studies (Murphy et al., 1997). Another possible effect of the LASAIR operating under saturation conditions is the possibility of more than one particle being in the optical sensing volume at the same time. This coincidence of particles may also cause an undercounting; in addition, it may shift the size distribution to larger sizes because the instrument may classify the particles in the sensing volume as a single larger particle.

The shapes of the size distributions in Fig. 8 are similar for large particle sizes, while the LASAIR detects fewer small particles than the AMS + BC + soil. This may partially be due to the larger size cut at the small end for the LASAIR, that nominally detects 50% of the particles between d_p=100–200 nm, compared to the AMS, which detects all (spherical) particles down to about 60 nm and has some transmission down to ∼33 nm (Zhang et al., 2004a). The agreement between the size distributions can be improved if the mass concentration in the smallest LASAIR channel is multiplied by two in order to account for the lower detection efficiency of the smallest particles, as it is shown by the dashed line in Fig. 8.

Another possible source for the apparent discrepancy is the presence of irregular soot particles that are sized smaller than their volume-equivalent diameter by the AMS (DeCarlo et al., 2004; Slowik et al., 2004; Zhang et al., 2005b) and likely sized larger by the LASAIR since light scattering is roughly proportional to particle surface area. A similar apparent discrepancy when comparing AMS and SMPS data for Pittsburgh is shown in Fig. 4a of Zhang et al. (2005b). An important piece of information arising from the LASAIR data is the relatively low mass concentrations of particles between 1 and 3 μm (even when the size distribution might be shifted to larger sizes as it was mentioned above). In some previous AMS studies the concentrations of particles in

this size range have been high, leading to significantly higher $PM_{2.5}$ than PM_1 mass concentrations (Zhang et al., 2005b). The fact that this is not the case during MCMA-2003 is consistent with the good agreement seen in Fig. 7 between the total AMS + BC + soil concentrations and those measured by the TEOM and DustTrak which operated

5 with $PM_{2.5}$ size cuts.

Figure 9 compares the time series of AMS + BC + soil mass concentrations with the estimated LASAIR mass concentrations. To estimate the LASAIR mass concentration shown in the figure, the size dependent density described above was used, and only the first six channels ($0.1\,\mu m$ to $1.0\,\mu m$ geometrical diameter) were considered be-

10 cause they correspond to approximately 137 nm to 1370 nm in vacuum aerodynamic diameter, which roughly corresponds to the size range that the AMS can measure.

It can be seen in Fig. 9 that the LASAIR measures about 43% of the mass concentration of AMS + BC + soil. However, both measurements capture similar dynamics and changes of the mass concentration in time (e.g. r^2=0.78). The absolute discrepancy is

15 likely due to saturation of the LASAIR with the high particle number concentrations in Mexico City.

Some air quality standards for fine particles are based on $PM_{2.5}$ total mass concentration. In Fig. 10 we present an estimation of the species contributions to the total average $PM_{2.5}$ mass concentration from the available particle composition data

20 at CENICA during MCMA-2003. PIXE analyses on the impactor substrates indicate that the average concentration of NaCl was at most $0.1\,\mu g\,m^{-3}$, and hence we did not include sodium in this figure or the previous analysis. Another species that we did not include is particulate water, because there are significant uncertainties in water quantification with the AMS due to evaporation losses in the inlet. Note that although water

25 evaporation in the AMS inlet has been observed by several groups, evaporation of other species is not believed to be a problem for AMS ambient measurements, since the vapor pressure of other aerosol components is typically at least 6–7 orders of magnitude below that of water. Finally, although the AMS measures NR-PM_1, LASAIR measurements during the MCMA-2003 campaign show that the particle mass in the range of

Print Version

Interactive Discussion

1–3 μm is small. For this reason, and to avoid double counting the BC and soil particulate mass in this size range, we did not include an estimation of the mass concentration of the NR particulate matter 1–2.5 μm. For comparison purposes, Fig. 10 also shows the average DustTrak PM$_{2.5}$ mass concentration for the same period. The difference between the estimated PM$_{2.5}$ from speciated measurements and the DustTrak PM$_{2.5}$ is within the experimental uncertainties; hence, we conclude that the combination of the AMS, BC, and soil particulate mass measurements can be used as an estimate of PM$_{2.5}$ during MCMA-2003, which is consistent with other particle measurements.

4. Conclusions

Two Aerodyne Aerosol Mass Spectrometers were deployed in Mexico City as part of the MCMA-2003 field campaign. The results of this deployment will be presented in a series of papers, of which this is the first one. Here we focus on the calibrations, measurement of shape-related collection efficiencies, and comparison of both AMSs with each other and with other collocated particle instruments. The calibration and sensitivity of the instruments were stable during the campaign, and the measured detection limits were similar to those reported for previous campaigns. For the first time, we report the use of a beam width probe inside an AMS during a field campaign to probe the surrogate shape and mixing state of the particles, and to quantify potential losses of irregular particles due to beam broadening. Results from this probe show that the shape-related collection efficiency of the particles was approximately one during the campaign. The speciation, and mass concentrations reported by the two AMSs compared well. The differences found are likely due to the different inlets used in both instruments. This is the first published intercomparison between two Q-AMSs. The combined AMS + BC + soil mass concentrations and size distribution are compared with other collocated instruments (LASAIR, TEOM, and DustTrak) and the results show that the combined AMS + BC + soil measurements represent a quantitative, size-resolved chemical speciation of the total PM$_{2.5}$ in MCMA. An overview of the dynamics

of these species during MCMA-2003 is presented in Part II of this series, with more detailed analysis to follow in future papers.

References

Alfarra, M. R., Coe, H., Allan, J. D., Bower, K. N., Boudries, H., Canagaratna, M. R., Jimenez, J. L., Jayne, J. T., Garforth, A., Li, S. M., and Worsnop, D. R.: Characterization of Urban and Regional Organic Aerosols In the Lower Fraser Valley Using Two Aerodyne Aerosol Mass Spectrometers, Atmos. Environ., 38, 5745–5758, 2004.

Allan, J. D., Jimenez, J. L., Coe, H., Bower, K. N., Williams, P. I., and Worsnop, D. R.: Quantitative Sampling Using an Aerodyne Aerosol Mass Spectrometer, Part 1: Techniques of Data Interpretation and Error Analysis, J. Geophys. Res., 108, 4090, doi:10.1029/2002JD002358, 2003.

Allan, J. D., Bower, K. N., Coe, H., Boudries, H., Jayne, J. T., Canagaratna, M. R., Millet, D. B., Goldstein, A. H., Quinn, P. K., Weber, R. J., and Worsnop, D. R.: Submicron aerosol composition at Trinidad Head, CA during ITCT 2K2, its relationship with gas phase volatile organic carbon and assessment of instrument performance, J. Geophys. Res., 109, doi:10.1029/2003JD004208, 2004a.

Allan, J. D., Delia, A. E., Coe, H., Bower, K. N., Alfarra, M. R., Jimenez, J. L., Middlebrook, A. M., Drewnick, F., Onasch, T. B., Canagaratna, M. R., Jayne, J. T., and Worsnop, D. R.:

Mexico City aerosol during MCMA-2003 using an AMS – Part I

D. Salcedo et al.

Title Page

Abstract	Introduction
Conclusions	References
Tables	Figures

Back Close

Full Screen / Esc

Print Version

Interactive Discussion

EGU

Technical note: A generalized method for the extraction of chemically resolved mass spectra from Aerodyne aerosol mass spectrometer data, J. Aerosol. Sci., 35, 909–922, 2004b.

Bahreini, R., Keywood, M. D., Ng, N. L., Varutbangkul, V., Gao, S., Flagan, R. C., Seinfeld, J. H., Worsnop, D. R., and Jimenez, J. L.: Measurements of Secondary Organic Aerosol (SOA) from oxidation of cycloalkenes, terpenes, and m-xylene using an Aerodyne Aerosol Mass Spectrometer, Environ. Sci. Technol., in press, 2005.

Baron, P. A. and Willeke, K.: Aerosol Measurement: Principles, Techniques, and Applications, Wiley-Interscience, Hoboken, NH, 2001.

Canagaratna, M. R., Jayne, J. T., Ghertner, D. A., Herndon, S., Shi, Q., Jimenez, J. L., Silva, P. J., Williams, P. I., Lanni, T., Drewnick, F., Demerjian, K. L., Kolb, C. E., and Worsnop, D. R.: Chase Studies of Particulate Emissions from in-use New York City Vehicles, Aerosol Sci. Technol., 38, 555–573, 2004.

DeCarlo, P. F., Slowik, J. G., Worsnop, D. R., Davidovits, P., and Jimenez, J. L.: Particle Morphology and Density Characterization by Combined Mobility and Aerodynamic Diameter Measurements, Part 1: Theory, Aerosol Sci. Technol., 38, 1185–1205, doi:10.1080/027868290903907, 2004.

Drewnick, F., Schwab, J. J., Jayne, J. T., Canagaratna, M. R., Worsnop, D. R., and Demerjian, K. L.: Measurement of Ambient Aerosol Composition During the PMTACS-NY 2001 Using an Aerosol Mass Spectrometer, Part I: Mass concentrations, Aerosol Sci. Technol., 38, 92–103, doi:10.1080/02786820390229507, 2004a.

Drewnick, F., Jayne, J. T., Canagaratna, M. R., Worsnop, D. R., and Demerjian, K. L.: Measurement of Ambient Aerosol Composition During the PMTACS-NY 2001 Using an Aerosol Mass Spectrometer, Part II: Chemically Speciated Mass Distributions, Aerosol Sci. Technol., 38, 104–117, 2004b.

Hansen, A. D. A., Rosen, H., and Novakov, T.: Real-time measurement of the absorption coefficient of aerosol particles, Appl. Optics, 21, 3060–3062, 1982.

Heberlein, J., Postel, O., Girshick, S., McMurry, P., Gerberich, W., Iordanoglou, D., Di Fonzo, F., Neumann, D., Gidwani, A., Fan, M., and Tymiak, N.: Thermal plasma deposition of nanophase hard coatings, Surf. Coat. Technol., 142, 265–271, 2001.

Hinds, W. C.: Aerosol technology; properties behavior, and measurement of airborne particles, John Wiley and Sons, USA, 1999.

Hogrefe, O., Schwab, J. J., Drewnick, F., Lala, G. G., Peters, S., Demerjian, K. L., Rhoads, K., Felton, H. D., Rattigan, O. V., Husain, L., and Dutkiewicz, V. A.: Semicontinuous PM2.5

Mexico City aerosol during MCMA-2003 using an AMS – Part I

D. Salcedo et al.

Title Page

Abstract	Introduction
Conclusions	References
Tables	Figures

◄ | ►

◄ | ►

Back | Close

Full Screen / Esc

Print Version

Interactive Discussion

Sulfate and Nitrate Measurements at an Urban and a Rural Location in New York: PMTACS-NY Summer 2001 and 2002 Campaigns, J. Air. Waste Manage., 54, 1040–1060, 2004.

Jayne, J. T., Leard, D. C., Zhang, X., Davidovits, P., Smith, K. A., Kolb, C. E., and Worsnop, D. R.: Development of an Aerosol Mass Spectrometer for Size and Composition Analysis of Submicron Particles, Aerosol Sci. Technol., 33, 49–70, 2000.

Jeong, C.-H., Hopke, P. K., Kim, E., and Lee, D.-W.: The comparison between thermal-optical transmittance elemental carbon and Aethalometer black carbon measured at multiple monitoring sites, Atmos. Environ., 38, 5193–5204, 2004.

Jimenez, J. L., Jayne, J. T., Shi, Q., Kolb, C. E., Worsnop, D. R., Yourshaw, I., Seinfeld, J. H., Flagan, R. C., Zhang, X., Smith, K. A., Morris, J., and Davidovits, P.: Ambient aerosol sampling using the Aerodyne Aerosol Mass Spectrometer, J. Geophys. Res., 108, 8425, doi:10.1029/2001JD001213, 2003a.

Jimenez, J. L., Bahreini, R., Cocker, D. R., Zhuang, H., Varutbangkul, V., Flagan, R. C., Seinfeld, J. H., O'Dowd, C. D., and Hoffmann, T.: New particle formation from photooxidation of diiodomethane (CH_2I_2), J. Geophys. Res., 108, 4318, doi:10.1029/2002JD002452, 2003b.

Jimenez, J. L., Bahreini, R., Cocker, D. R., Zhuang, H., Varutbangkul, V., Flagan, R. C., Seinfeld, J. H., O'Dowd, C. D., and Hoffmann, T.: Correction to "New particle formation from photooxidation of diiodomethane (CH_2I_2)", J. Geophys. Res., 108, 4733, doi:10.1029/2003JD004249, 2003c.

Johnson, K. S., Zuberi, B., Iedema, M. J., Cowin, J. P., Gaspar, D. J., Wang, C., Laskin, A., Molina, L. T., and Molina, M. J.: Processing of Soot in an Urban Environment: Case Study from the Mexico City Metropolitan Area, Atmos. Chem. Phys. Discuss., accepted, 2005b.

Katrib, Y., Martin, S. T., Rudich, Y., Davidovits, P., Jayne, J. T., and Worsnop, D. R.: Density Changes of Aerosol Particles as a Result of Chemical Reaction, Atmos. Chem. Phys., 5, 275–291, 2005,
SRef-ID: 1680-7324/acp/2005-5-275.

Kolb, C. E., Herndon, S. C., McManus, J. B., Shorter, J. H., Zahniser, M. S., Nelson, D. D., Jayne, J. T., Canagaratna, M. R., and Worsnop, D. R.: Mobile Laboratory with Rapid Response Instruments for Real-Time Measurements of Urban and Regional Trace Gas and Particulate Distributions and Emission Source Characteristics, Environ. Sci. Technol., 38, 5694–5703, 2004.

Lide, D. R.: CRC Handbook of Chemistry and Physics, CRC Press Inc, USA, 1991.

Liu, P., Ziemann, P. J., Kittelson, D. B., and McMurry, P. H.: Generating particle beams of

EGU

controlled dimensions and divergence. 2. Experimental evaluation of particle motion in aerodynamic lenses and nozzle expansions, Aerosol Sci. Technol., 22, 314–324, 1995.

Malm, W. C., Sisler, J. F., Huffman, D., Eldred, R. A., and Cahil, T. A.: Spatial and seasonal trends in particle concentration and optical extinction in the United States, J. Geophys. Res., 99, 1347–11370, 1994.

Marley, N. A., Gaffney, J. S., Baird, J. C., Blazer, C. A., Drayton, P. J., and Frederick, J. E.: The determination of scattering and absorption coefficients of size-fractionated aerosols for radiative transfer calculations, Aerosol Sci. Technol., 34, 535–549, 2001.

Maxwell, J. A., Campbell, J. L., and Teesdale, W. J.: The Guelph-PIXE software package-II, Nucl. Instrum. Methods Phys. Res. B, 3, 407–421, 1995.

Murphy, D. M., Thomson, D. S., Kaluzhny, M., Marti, J. J., and Weber, R. J.: Aerosol characteristics at Idaho Hill during the OH Photochemistry Experiment, J. Geophys. Res., 102, 6325–6330, 1997.

Park, K., Kittelson, D. B., Zachariah, M. R., and McMurry, P. H.: Measurement of Inherent Material Density of Nanoparticle Agglomerates, J. Nanopart. Res., 6, 267–272, 2004.

Salcedo, D., Dzepina, K., Onasch, T. B., Canagaratna, M. R., Jayne, J. T., Worsnop, D. R., Gaffney, J. S., Marley, N. A., Johnson, K. S., Zuberi, B., Shutthanandan, V., Molina, L. T., Molina, M. J., and Jimenez, J. L.: Characterization of Ambient Aerosols in Mexico City during the MCMA-2003 Campaign with Aerosol Mass Spectrometry – Part II: Overview of the Results at the CENICA Supersite and Comparison to Previous Studies, Atmos. Chem. Phys. Discuss., 5, 4183–4221, 2005
SRef-ID: 1680-7375/acpd/2005-5-4183.

Shutthanandan, V., Thevuthasan, S., Disselkamp, R., Stroud, A., Cavanagh, A., Adams, E. M., Baer, D. R., Barrie, L. A., Cliff, S. S., Jimenez-Cruz, M., and Cahill, T. A.: Development of PIXE, PESA and transmission ion microscopy capability to measure aerosols by size and time, Nucl. Instrum. Methods Phys. Res. B, 189, 284–288, 2002.

Slowik, J. G., Stainken, K., Davidovits, P., Williams, L. R., Jayne, J. T., Kolb, C. E., Worsnop, D. R., Rudich, Y., DeCarlo, P., and Jimenez, J. L.: Particle Morphology and Density Characterization by Combined Mobility and Aerodynamic Diameter Measurements. Part 2: Application to combustion Generated Soot Aerosols as a Function of Fuel Equivalence Ratio, Aerosol Sci. Technol., 38, 1206–1222, 2004.

TSI: DUSTTRAK™Aerosol Monitor Theory of Operation, TSI incorporated, St. Paul, MN, 2004.

Mexico City aerosol during MCMA-2003 using an AMS – Part I

D. Salcedo et al.

EGU

Turpin, B. J. and Lim, H.-J.: Species Contributions to PM2.5 Mass Concentrations: Revisiting Common Assumptions for Estimating Organic Mass, Aerosol Sci. Technol., 35, 602–610, 2001.

Zhang, X., Smith, K. A., Worsnop, D. R., Jimenez, J. L., Jayne, J. T., and Kolb, C. E.: A Numerical Characterization of Particle Beam Collimation by an Aerodynamic Lens-Nozzle System. Part I: An Individual Lens or Nozzle, Aerosol Sci. Technol., 36, 617–631, 2002.

Zhang, Q., Stanier, C. O., Canagaratna, M. R., Jayne, J. T., Worsnop, D. R., Pandis, S. N., and Jimenez, J. L.: Insights into the Chemistry of New Particle Formation and Growth Events in Pittsburgh Based on Aerosol Mass Spectrometry, Environ. Sci. Technol., 38, 4797–4809, 2004a.

Zhang, X., Smith, K. A., Worsnop, D. R., Jimenez, J. L., Jayne, J. T., Kolb, C. E., Morris, J., and Davidovits, P.: Characterization of Particle Beam Collimation. Part II: Integrated Aerodynamic Lens-Nozzle System, Aerosol Sci. Technol., 38, 619–638, 2004b.

Zhang, Q., Alfarra, M. R., Worsnop, D. R., Allan, J. D., Coe, H., Canagaratna, M. R., and Jimenez, J. L.: Deconvolution and Quantification of Primary and Oxygenated Organic Aerosols Based on Aerosol Mass Spectrometry. Part 1: Development and Validation of the Method, Environ. Sci. Technol., doi:10.1021/es048568l, 2005a.

Zhang, Q., Canagaratna, M. R., Jayne, J. T., Worsnop, D. R., and Jimenez, J. L.: Time and Size-Resolved Chemical Composition of Submicron Particles in Pittsburgh, Implications for Aerosol Sources and Processes, J. Geophys. Res., 110, doi:10.1029/2004JD004649, 2005b.

Title Page

Abstract | Introduction

Conclusions | References

Tables | Figures

◄ | ►

◄ | ►

Back | Close

Full Screen / Esc

Print Version

Interactive Discussion

EGU
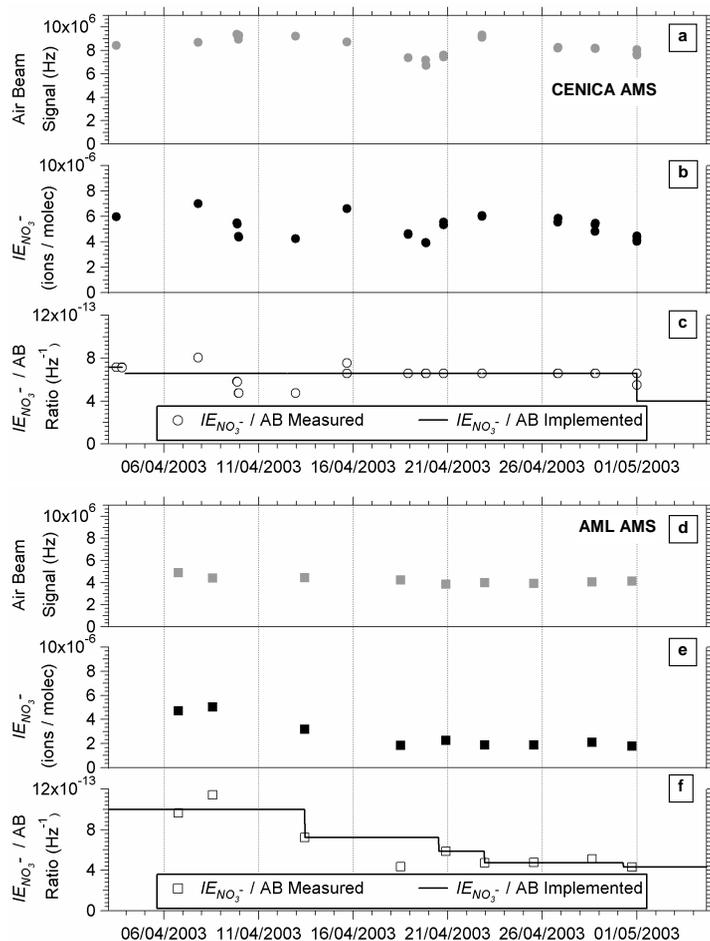
Fig. 1. Summary of the results of the ionization efficiency calibrations of the CENICA (panels **a**–**c**) and Mobile Laboratory (panels **d**–**f**) AMSs during the MCMA-2003 field campaign.

EGU
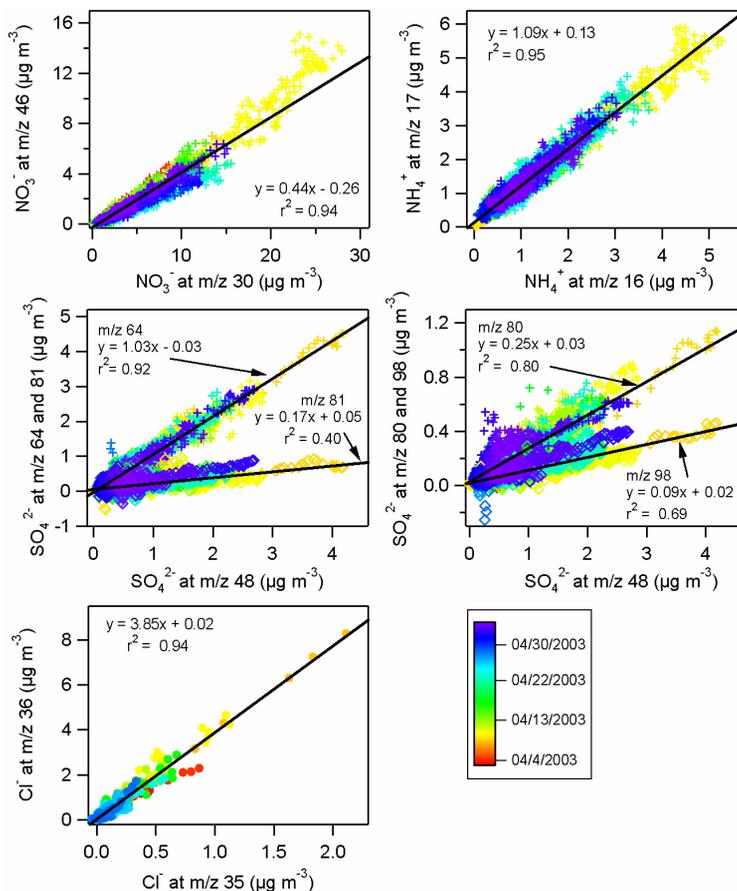
Fig. 2. Correlations between the time series of the main fragments used to calculate mass concentration of the inorganic species for the CENICA AMS. Black lines are linear fits to the data.

EGU
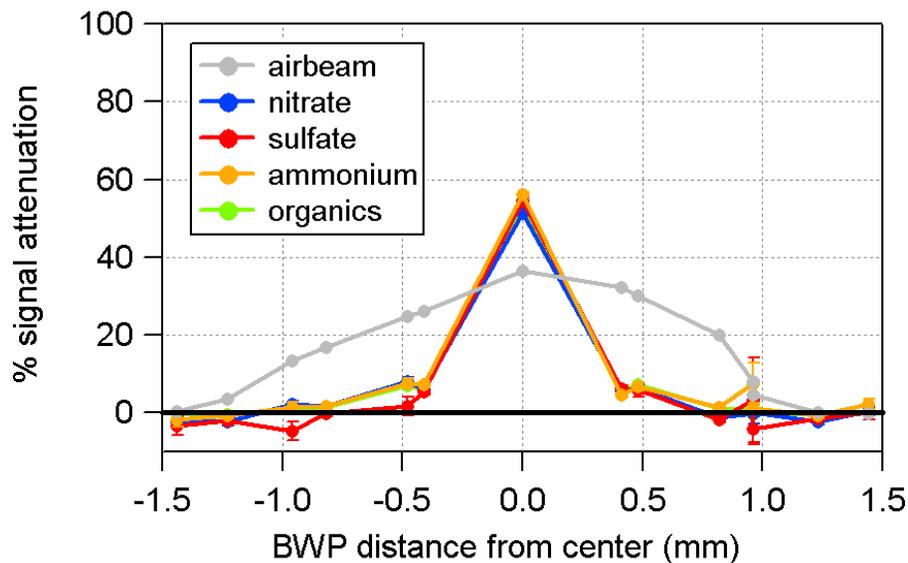
Fig. 3. Campaign-average signal attenuation for the airbeam and the main CENICA AMS species as a function of distance of the BWP from the center of the vaporizer. Nitrate, sulfate, and organics curves are not visible because they are behind the ammonium curve.

ACPD

5, 4143–4182, 2005

Mexico City aerosol during MCMA-2003 using an AMS – Part I

D. Salcedo et al.

Title Page	
Abstract	Introduction
Conclusions	References
Tables	Figures
◀	▶
◀	▶
Back	Close
Full Screen / Esc	

Print Version

Interactive Discussion

EGU
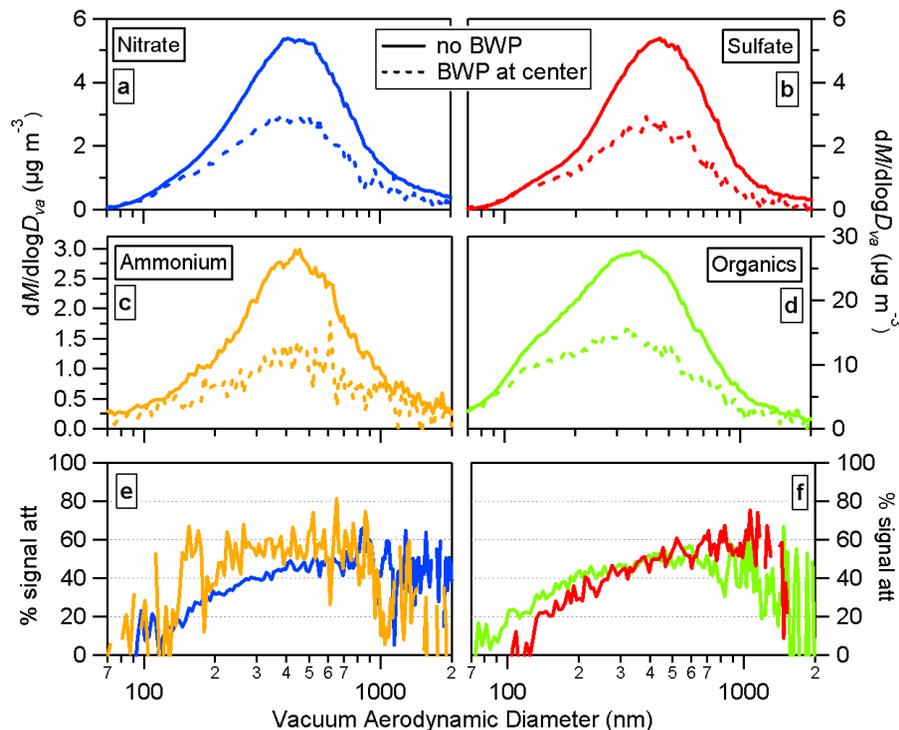
Fig. 4. Panels **(a)** through **(d)**: Campaign-average size distributions obtained by the CENICA AMS without the BWP and with the BWP blocking the particle beam at the center position. Panels **(e)** and **(f)**: signal attenuation caused by the BWP at the center position as a function of particle size.
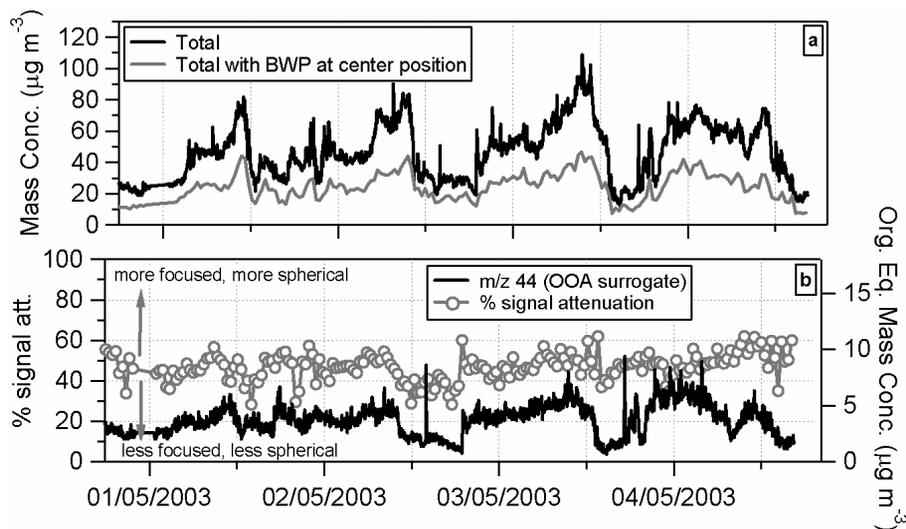
Fig. 5. Panel **(a)**: time series of the AMS Total mass concentration (when the beam width probe (BWP) was in the "out position"), and the mass concentration measured when the BWP was blocking the particle beam at the center position. Panel **(b)**: signal attenuation caused by the BWP at the center position, and time series of the AMS fragment m/z 44 (marker for oxygenated organics (OOA)) in Org. Eq. Mass Concentration. The mass concentrations in this graph were not corrected for air beam variations.
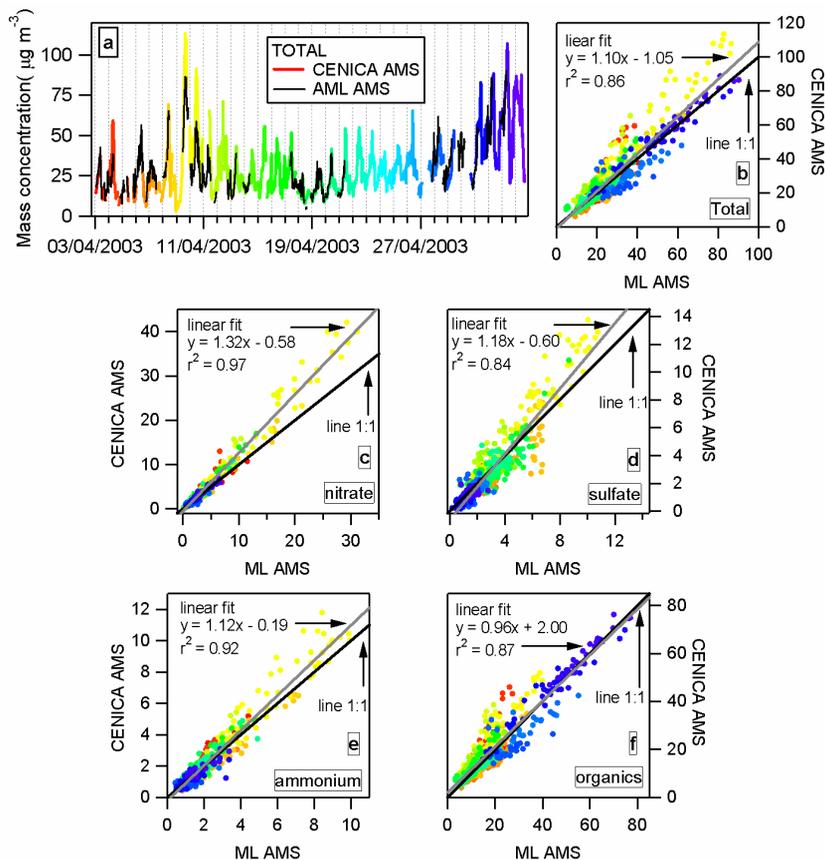
Fig. 6. Panel **(a)**: comparison of the time series of Total NR-PM$_1$ measured with the CENICA and the mobile laboratory AMSs, for periods when the AML was parked at CENICA during MCMA-2003. Panels **(b)** though **(f)**: scatter plots of the Total NR-PM$_1$, and its species, measured with the CENICA and the mobile laboratory AMSs. Black lines are 1:1 lines. Grey lines are linear fits to the data. The data is presented in 30 min averages.

EGU
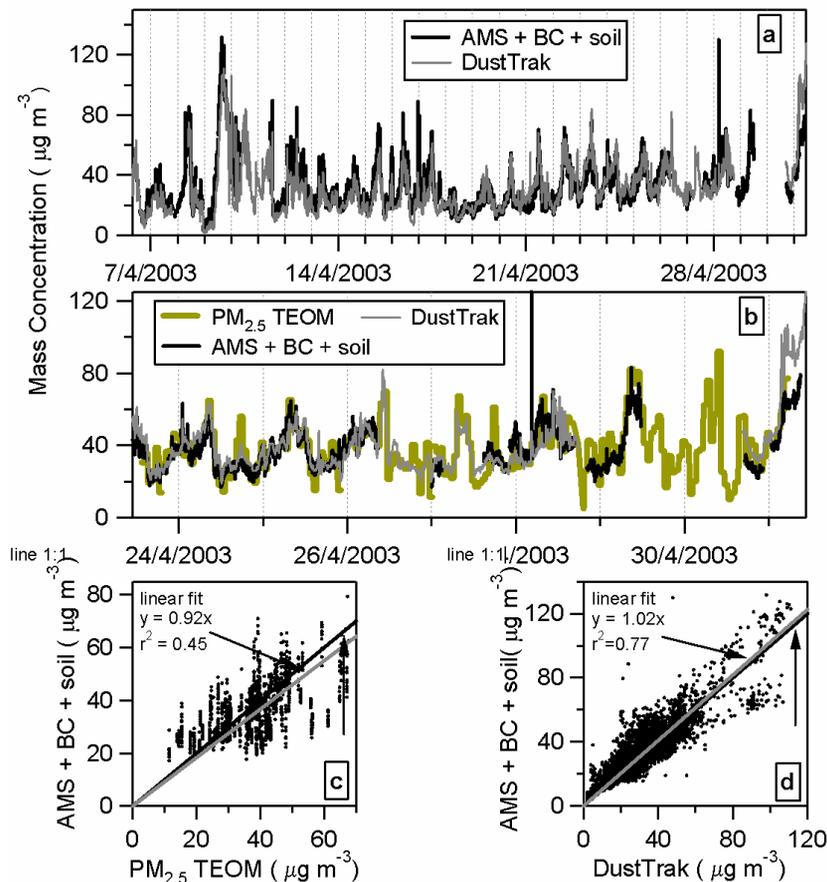
Fig. 7. Panels **(a)** and **(b)**: comparison of the time series of the AMS + BC + soil with DustTrak and TEOM $PM_{2.5}$ mass concentrations. Panels **(c)** and **(d)**: scatter plots and linear fits for the above comparisons. Grey lines are linear fits to the data.

Fig. 8. Comparison of the (AMS + estimated BC + soil) and LASAIR size distributions. The BC, AMS and soil size distributions are stacked. The dashed line represents the mass concentration of the smallest LASAIR size channel multiplied by two in order to account for the 50% collection efficiency in this channel.
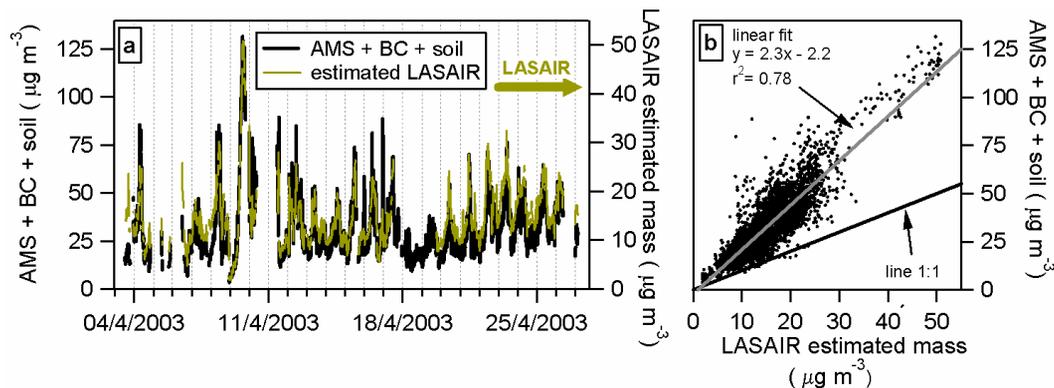
Fig. 9. Panel **(a)**: Comparison of the time series of the AMS + BC + soil mass concentration and the estimated mass concentration from the LASAIR instrument. Panel **(b)**: scatter plot and linear fit between both measurements. The grey line is a linear fit to the data.

Title Page

Abstract | Introduction

Conclusions | References

Tables | Figures

◀ | ▶

◀ | ▶

Back | Close

Full Screen / Esc

Print Version

Interactive Discussion

Print Version

Interactive Discussion

EGU
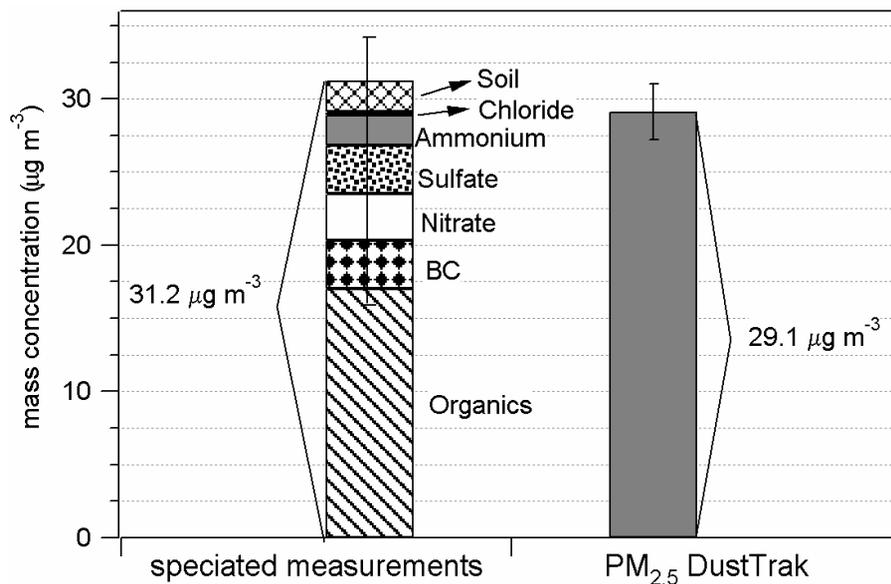
Fig. 10. Estimation of the total PM$_{2.5}$ mass concentration from AMS, BC, and soil mass concentration, compared with PM$_{2.5}$ DustTrak mass concentration. Averages were carried out over all time intervals for which all data (AMS, BC, soil, and DustTrak) were available.